4288 *Inorg. Chem.* **2010**, *49*, 4288–4300
DOI: 10.1021/ic100165t

Inorganic Chemistry
Article

Coordinatively Diverse *ortho*-Phosphinoaniline Complexes of Ruthenium and Isolation of a Putative Intermediate in Ketone Transfer Hydrogenation Catalysis

Lindsay J. Hounjet, Matthias Bierenstiel,[†] Michael J. Ferguson,[‡] Robert McDonald,[‡] and Martin Cowie*

Department of Chemistry, University of Alberta, Edmonton, Alberta, Canada T6G 2G2.
[†]Present Address: Department of Chemistry, Cape Breton University, Sydney, Nova Scotia, Canada, B1P 6L2.
[‡]X-ray Crystallography Laboratory, University of Alberta

Received January 26, 2010

Amine-functionalized mono- and diphosphines have been used to prepare a series of ruthenium complexes which exhibit a variety of coordination modes depending on the number of donors possessed by the ligands, the degree of amine methylation, the solvent system used, and the oxidation state of the metal. Reactions of the monophosphinoanilines, Ph_2PAr or Ph_2PAr' (Ar = *o*-C_6H_4NHMe, Ar′ = *o*-$C_6H_4NMe_2$), with 0.5 equiv of $[RuCl(\mu\text{-}Cl)(\eta^6\text{-}p\text{-cymene})]_2$ in dichloromethane result in the formation of $[RuCl_2(\eta^6\text{-}p\text{-cymene})(P\text{-}Ph_2PAr)]$ or $[RuCl(\eta^6\text{-}p\text{-cymene})(P,N\text{-}Ph_2PAr')]Cl$, respectively. In refluxing methanol, $[RuCl_2(\eta^6\text{-}p\text{-cymene})(P\text{-}Ph_2PAr)]$ gradually undergoes chloride ion dissociation to afford the *P*,*N*-chelate, $[RuCl(\eta^6\text{-}p\text{-cymene})(P,N\text{-}Ph_2PAr)]Cl$. This chelate can then be deprotonated to afford the amido complex, $[RuCl(\eta^6\text{-}p\text{-cymene})(P,N\text{-}Ph_2PAr^-)]$ (Ar^- = *o*-$C_6H_4NMe^-$), which is an active ketone transfer hydrogenation catalyst. Reactions of the diphosphines, $Ar_2PCH_2PAr_2$ (mapm) or $Ar'_2PCH_2PAr'_2$ (dmapm) with 0.5 equiv of $[RuCl(\mu\text{-}Cl)(\eta^6\text{-}p\text{-cymene})]_2$ result in the formation of $[RuCl_2(P,P',N,N'\text{-mapm})]$ or $[RuCl(\eta^6\text{-}p\text{-cymene})(P,P'\text{-dmapm})]Cl$, respectively, in which increased methyl substitution in the latter actually inhibits amine coordination with retention of the *p*-cymene fragment. Reaction of mapm with 1 equiv of $[Ru(CO)_4(\eta^2\text{-}C_2H_4)]$ in dichloromethane initially produces $[Ru(CO)_4(P\text{-mapm})]$ which, over a 24 h period with exposure to ambient light, is completely converted to the *P*,*P*′-chelate, $[Ru(CO)_3(P,P'\text{-mapm})]$, by photodissociation of carbon monoxide. The same reaction with 2 equiv of $[Ru(CO)_4(\eta^2\text{-}C_2H_4)]$ generates a mixture of $[Ru_3(CO)_{10}(\mu\text{-}P,P'\text{-mapm})]$ and the mononuclear *P*,*P*′-chelate. The trinuclear complex can also be synthesized by direct reaction of mapm with 1 equiv of $[Ru_3(CO)_{12}]$.

Introduction

Hybrid ligands, which contain more than one type of donor functionality, have attracted much recent interest.[1−5] The incorporation of two or more different donor groups can result in coordinatively diverse complexes because of the steric and electronic asymmetries[6] that are introduced by the mixed-donor ligands upon coordination. Furthermore, when the differing donor atoms are electronically diverse hard and soft combinations, the additional aspect of hemilability[7] can come into play. *P*,*N*-Ligands bearing soft phosphine and hard amine donors can provide a unique electronic environment for the metal center, in which the weakly π-acidic character of the phosphine is coupled with the σ-donor character of the amine.[5,6] The hybrid electronic characteristics of ruthenium *P*,*N*-complexes have been exemplified by their highly variable stereochemistries[8−13] and such complexes have found many applications as catalysts for (transfer) hydrogenation,[11−16] hydroformylation,[17,18] hydrosilylation,[19,20] and terminal alkyne homocoupling[21] reactions.

*To whom correspondence should be addressed. E-mail: martin.cowie@ualberta.ca. Fax: 01 7804928231. Phone: 01 7804925581.

(1) Braunstein, P.; Naud, F. *Angew. Chem., Int. Ed.* **2001**, *40*, 680–699.
(2) Slone, C. S.; Weinberger, D. A.; Mirkin, C. A. *Prog. Inorg. Chem.* **1999**, *48*, 233–350.
(3) Werner, H. *Dalton Trans.* **2003**, 3829–3837.
(4) Lindner, E.; Pautz, S.; Haustein, M. *Coord. Chem. Rev.* **1996**, *155*, 145–162.
(5) Espinet, P.; Soulantica, K. *Coord. Chem. Rev.* **1999**, *193−195*, 499–556.
(6) Guiry, P. J.; Saunders, C. P. *Adv. Synth. Catal.* **2004**, *346*, 497–537.
(7) Jeffrey, J. C.; Rauchfuss, T. B. *Inorg. Chem.* **1979**, *18*, 2658–2666.
(8) Dabb, S. L.; Messerle, B. A.; Smith, M. K.; Willis, A. C. *Inorg. Chem.* **2008**, *47*, 3034–3044.
(9) Ziessel, R.; Toupet, L.; Chardon-Noblat, S.; Deronzier, A.; Matt, D. *J. Chem. Soc., Dalton Trans.* **1997**, 3777–3784.
(10) Costella, L.; Del Zotto, A.; Mezzetti, A.; Zangrando, E.; Rigo, P. *J. Chem. Soc., Dalton Trans.* **1993**, 3001–3008.
(11) Braunstein, P.; Graiff, C.; Naud, F.; Pfaltz, A.; Tiripicchio, A. *Inorg. Chem.* **2000**, *39*, 4468–4475.
(12) Yang, H.; Alvarez-Gressier, M.; Lugan, N.; Mathieu, R. *Organometallics* **1997**, *16*, 1401–1409.
(13) Dahlenburg, L.; Kühnlein, C. *J. Organomet. Chem.* **2005**, *690*, 1–13.
(14) Braunstein, P.; Naud, F.; Rettig, S. J. *New J. Chem.* **2001**, *25*, 32–39.
(15) Rahman, M. S.; Prince, P. D.; Steed, J. W.; Hii, K. K. *Organometallics* **2002**, *21*, 4927–4933.
(16) Bacchi, A.; Balordi, M.; Cammi, R.; Elviri, L.; Pelizzi, C.; Picchioni, F.; Verdolino, V.; Goubitz, K.; Peschar, R.; Pelagatti, P. *Eur. J. Inorg. Chem.* **2008**, 4462–4473.
(17) Moreno, M. A.; Haukka, M.; Jääskeläinen, S.; Vuoti, S.; Pursiainen, J.; Pakkanen, T. A. *J. Organomet. Chem.* **2005**, *690*, 3803–3814.

 Published on Web 04/05/2010

Hybrid *P*,*N*-chelate complexes which exhibit hemilability are of particular interest in homogeneous catalysis by low-valent, late-metal complexes[12,14] in which the labile amine can be readily displaced by the catalytic substrate and, after completion of the metal-mediated transformation, can facilitate decomplexation of the modified substrate by recoordination, thereby stabilizing the catalyst. Recently, we demonstrated how the rate of hemilabile, internal ligand exchange processes within *ortho*-phosphinoaniline complexes of rhodium(I) can be varied by exploiting steric requirements of the amines via the degree of *N*-methyl substitution.[22]

In the current study, we illustrate how the degree of *N*-methylation and the number of available phosphine and amine donors substantially diversifies the coordination behavior of these ligands at ruthenium, but surprisingly, does not give rise to observable hemilability in the compounds studied. A further motivation for the study of incompletely substituted amines as donors to ruthenium stems from the well-documented "N−H effect,"[23] in which the amine can be deprotonated by the addition of an external base to generate amido-ruthenium complexes, many of which function as catalytic intermediates for the (transfer) hydrogenation of polar substrates, particularly ketones.[23,24] Recently, Stradiotto et al. reported efficient "non-N−H" iridium-based transfer hydrogenation catalysts bearing an *o*-*N*,*N*-dimethylanilinylphosphine ligand,[25] while Pelagatti et al. also demonstrated transfer hydrogenation using the same ligand within a ruthenium complex.[16] Ruthenium complexes possessing other types of NMe_2-containing donor ligands have also been shown to act as catalysts for ketone transfer hydrogenation reactions.[26,27] Such examples serve to illustrate the catalytic utility of completely *N*-substituted *ortho*-phosphinoaniline complexes. Interestingly, *P*,*N*-ligated ruthenium(II)-arene complexes have also received attention as selective anticancer agents.[28]

Experimental Section

General Comments. All solvents were deoxygenated, dried (using appropriate drying agents), distilled before use, and stored under nitrogen. All reactions were performed under an Ar atmosphere using standard Schlenk techniques. The reagents, $[Ru_3(CO)_{12}]$, $[RuCl(\mu\text{-}Cl)(\eta^6\text{-}p\text{-cymene})]_2$ (**1**), and triethylamine were purchased from Strem Chemicals. Isopropanol (>99%, distilled over Mg turnings and stored under Ar), acetophenone (99%, deoxygenated and stored under Ar over 5 Å molecular sieves), and potassium *tert*-butoxide (resublimed and stored under Ar), used for transfer hydrogenation catalysis, were purchased from Aldrich. Ethylene was purchased from Matheson Tri-Gas. Diphenyl(*o*-*N*,*N*-dimethylanilinyl)phosphine (Ph_2PAr'),[29] bis(di(*o*-*N*,*N*-dimethylanilinyl)phosphino)methane (dmapm),[30] diphenyl(*o*-*N*-methylanilinyl)phosphine (Ph_2PAr),[22] and bis(di(*o*-*N*-methylanilinyl)phosphino)methane (mapm)[22] were prepared as previously reported. NMR spectra were recorded on Varian Inova-400, -500 or Varian Unity-500 spectrometers operating at 399.8, 498.1, or 499.8 MHz, respectively, for ^1H, at 161.8, 201.6, or 202.3 MHz, respectively, for ^{31}P and at 100.6, 125.3, or 125.7 MHz, respectively, for ^{13}C nuclei. *J* values are given in hertz (Hz) and overlapping or unresolved aromatic ^1H signals, observed in the typical 6−8 ppm range, and $^{13}C\{^1H\}$ signals, found between 80−120 ppm, respectively, are not reported. Spectroscopic data for all metal complexes (**2a**−**c**, **3b**, **4**, **5**, **6a**, **6b**, and **7**) are provided in Table 1. Solution phase infrared spectra (KBr cell) were recorded on a FT-IR Bomem MB-100 spectrometer. Elemental analyses were performed by the Microanalytical Laboratory of the University of Alberta. Electrospray ionization mass spectra were run on a Micromass Zabspec spectrometer in the departmental MS facility. In all cases, the distribution of isotope peaks for the appropriate parent ion matched very closely that calculated from the formulation given. Conductivity measurements were carried out under inert conditions on 10^{-3} M solutions of $[RuCl_2(\eta^6\text{-}p\text{-cymene})(P\text{-}Ph_2PAr)]$ (**2a**), $[RuCl(\eta^6\text{-}p\text{-cymene})(P,N\text{-}Ph_2PAr)]Cl$ (**2b**), $[RuCl(\eta^6\text{-}p\text{-cymene})(P,N\text{-}Ph_2PAr^-)]$ (**2c**), $[RuCl(\eta^6\text{-}p\text{-cymene})(P,N\text{-}Ph_2PAr')]Cl$ (**3b**), $[RuCl(\eta^6\text{-}p\text{-cymene})(P,P'\text{-dmapm})]Cl$ (**4**), and $[RuCl_2(P,P',N,N'\text{-mapm})]$ (**5**) in dry nitromethane using a Yellow Springs Instrument Model 31 conductivity bridge. For these species the molar conductivities were determined as Λ = 6, 59, 23, 79, 62, and 7 $cm^2\ \Omega^{-1}\ mol^{-1}$, respectively.

Preparation of Metal Complexes. (a). Dichloro(η^6-*p*-cymene)-(diphenyl(*o*-*N*-methylanilinyl)phosphine)ruthenium(II), [$RuCl_2(\eta^6$-*p*-cymene)(*P*-Ph_2PAr)] (2a). Method i. In a 50 mL Schlenk flask under anhydrous conditions and Ar atmosphere, $[RuCl(\mu\text{-}Cl)(\eta^6\text{-}p\text{-cymene})]_2$ (**1**) (109 mg, 178 μmol) and Ph_2PAr (104 mg, 356 μmol) were dissolved in 15 mL of benzene at ambient temperature. The resulting red solution was stirred at ambient temperature for 30 min, and a bright red precipitate formed. The solvent was then removed in vacuo, and the red solid was washed with 15 mL of *n*-pentane. The solid was then dried in vacuo producing an orange-red powder (219 mg, 91% yield, found: C, 62.24; H, 6.10; N, 2.04%. Calcd for $[C_{29}H_{32}Cl_2NPRu]\cdot C_6H_6$: C, 62.22; H, 5.67; N, 2.07%). Although the crystal structure determination indicated no solvent inclusion, the sample used for elemental analysis was non-crystalline, and ^1H NMR analysis of this sample in CD_2Cl_2 (obtained at approximately the same time as the elemental analysis) verified the benzene content. Single crystals suitable for X-ray crystallographic analysis were obtained by dissolving the complex, under Ar atmosphere, in a minimum volume of benzene and layering the solution with anhydrous *n*-pentane in an NMR tube. HRMS (ESI): *m*/*z* 598.0760 $[M + H]^+$. Calcd for $C_{29}H_{33}Cl_2NPRu$: *m*/*z* 598.0766.

Method ii. Using dichloromethane rather than benzene, the product did not spontaneously precipitate, but was obtained in excellent yield by precipitation with ether and subsequent

(18) Drommi, D.; Nicolò, F.; Arena, C. G.; Bruno, G.; Faraone, F.; Gobetto, R. *Inorg. Chim. Acta* **1994**, *221*, 109–116.
(19) Zhu, G.; Terry, M.; Zhang, X. *J. Organomet. Chem.* **1997**, *547*, 97–101.
(20) Tuttle, T.; Wang, D.; Thiel, W.; Köhler, J.; Hofmann, M.; Weis, J. *Dalton Trans.* **2009**, 5894–5901.
(21) Slugovc, C.; Doberer, D.; Gemel, C.; Schmid, R.; Kirchner, K.; Winkler, B.; Stelzer, F. *Monatsh. Chem.* **1998**, *129*, 221–233.
(22) Hounjet, L. J.; Bierenstiel, M.; Ferguson, M. J.; McDonald, R.; Cowie, M. *Dalton Trans.* **2009**, 4213–4226.
(23) Clapham, S. E.; Hadzovic, A.; Morris, R. H. *Coord. Chem. Rev.* **2004**, *248*, 2201–2237.
(24) (a) Noyori, R.; Ohkuma, T. *Angew. Chem., Int. Ed.* **2001**, *40*, 40–73. (b) Haack, K.-J.; Hashiguchi, S.; Fujii, A.; Ikariya, T.; Noyori, R. *Angew. Chem., Int. Ed. Engl.* **1997**, *36*, 285–288. (c) Yamakawa, M.; Ito, H.; Noyori, R. *J. Am. Chem. Soc.* **2000**, *122*, 1466–1478.
(25) Lundgren, R. J.; Stradiotto, M. *Chem.—Eur. J.* **2008**, *14*, 10388–10395.
(26) Lundgren, R. J.; Rankin, M. A.; McDonald, R.; Schatte, G.; Stradiotto, M. *Angew. Chem., Int. Ed.* **2007**, *46*, 4732–4735.
(27) Standfest-Hauser, C.; Slugovc, C.; Mereiter, K.; Schmid, R.; Kirchner, K.; Xiao, L.; Weissensteiner, W. *J. Chem. Soc., Dalton Trans.* **2001**, 2989–2995.
(28) (a) Renfrew, A. K.; Phillips, A. D.; Egger, A. E.; Hartinger, C. G.; Bosquain, S. S.; Nazarov, A. A.; Keppler, B. K.; Gonsalvi, L.; Peruzzini, M.; Dyson, P. J. *Organometallics* **2009**, *28*, 1165–1172. (b) Bugarcic, T.; Habtemariam, A.; Deeth, R. J.; Fabbiani, F. P. A.; Parsons, S.; Sadler, P. J. *Inorg. Chem.* **2009**, *48*, 9444–9453.
(29) Fritz, H. P.; Gordon, I. R.; Schwarzhans, K. E.; Venanzi, L. M. *J. Chem. Soc.* **1965**, 5210–5216.
(30) Jones, N. D.; Meessen, P.; Smith, M. B.; Losehand, U.; Rettig, S. J.; Patrick, B. O.; James, B. R. *Can. J. Chem.* **2002**, *80*, 1600–1606.
(31) Cooke, J.; Berry, D. E.; Fawkes, K. L. *J. Chem. Educ.* **2007**, *84*, 115–118.

Table 1. NMR Spectroscopic Data for the Compounds[a]

compound	$\delta(^{31}P\{^1H\})$/ppm[b]	$\delta(^1H)$/ppm[c]	$\delta(^{13}C\{^1H\})$/ppm[c]
[$RuCl_2(\eta^6$-*p*-cymene)-(*P*-Ph_2PAr)] (**2a**)	28.2 (s, 1P)	N*H*: 5.47 (q/br, $^3J_{HH}$ = 5.0 Hz, 1H) C*H*(CH_3)$_2$: 3.08 (sept, $^3J_{HH}$ = 7.0 Hz, 1H) NC*H*$_3$: 2.81 (d, $^3J_{HH}$ = 5.0 Hz, 3H) ArC*H*$_3$: 1.84 (s, 3H) CH(C*H*$_3$)$_2$: 1.39 (d, $^3J_{HH}$ = 7.0 Hz, 6H)	*C*H(CH_3)$_2$: 30.9 (s) N*C*H$_3$: 30.3 (s) CH(*C*H$_3$)$_2$: 22.0 (s/br) Ar*C*H$_3$: 18.1 (s) CH(*C*H$_3$)$_2$: 24.3 (s); 19.6 (s)[g]
[$RuCl(\eta^6$-*p*-cymene)-(*P*,*N*-Ph_2PAr)]Cl (**2b**)	53.4 (s, 1P)	N*H*: 10.8 (m/br, 1H) NC*H*$_3$: 3.52 (d, $^3J_{HH}$ = 4.4 Hz, 3H) C*H*(CH_3)$_2$: 2.91 (sept, $^3J_{HH}$ = 7.0 Hz, 1H) ArC*H*$_3$: 1.36 (s, 3H) CH(C*H*$_3$)$_2$: 1.33 (d, $^3J_{HH}$ = 7.0 Hz, 3H); 1.31 (d, $^3J_{HH}$ = 7.0 Hz, 3H)	N*C*H$_3$: 76.7 (s) *C*H(CH_3)$_2$: 31.5 (s) CH(*C*H$_3$)$_2$: 22.7 (s); 20.5 (s) Ar*C*H$_3$: 15.6 (s)
[$RuCl(\eta^6$-*p*-cymene)-(*P*,*N*-Ph_2PAr^-)] (**2c**)	59.3 (s, 1P)	NC*H*$_3$: 3.52 (s, 3H) C*H*(CH_3)$_2$: 2.39 (sept, $^3J_{HH}$ = 6.8 Hz, 1H) ArC*H*$_3$: 2.09 (s, 3H) CH(C*H*$_3$)$_2$: 1.14 (s/br, 3H); 0.99 (s/br, 3H)	N*C*H$_3$: 48.6 (s) *C*H(CH_3)$_2$: 31.2 (s) CH(*C*H$_3$)$_2$: 22.4 (s) Ar*C*H$_3$: 18.3 (s)
[$RuCl(\eta^6$-*p*-cymene)-(*P*,*N*-Ph_2PAr')]Cl (**3b**)	47.5 (s, 1P)	N(C*H*$_3$)$_2$: 4.04 (s, 3H); 3.50 (s, 3H) C*H*(CH_3)$_2$: 2.87 (sept, $^3J_{HH}$ = 7.0 Hz, 1H) ArC*H*$_3$: 1.36 (s, 3H) CH(C*H*$_3$)$_2$: 1.35 (d, $^3J_{HH}$ = 7.0 Hz, 3H); 1.26 (d, $^3J_{HH}$ = 7.0 Hz, 3H)	N(*C*H$_3$)$_2$: 65.2 (s); 58.4 (s) *C*H(CH_3)$_2$: 31.7 (s) CH(*C*H$_3$)$_2$: 22.3 (s); 20.7 (s) Ar*C*H$_3$: 15.5 (s)
[$RuCl(\eta^6$-*p*-cymene)-(*P*,*P*′-dmapm)]Cl (**4**)	−1.5 (s, 2P)[d], 1.5 (d/br, $^2J_{PP}$ = 56 Hz, 1P)[e], −15.4 (d/br, $^2J_{PP}$ = 56 Hz, 1P)[e]	C*H*$_2$: 5.09 (m/br, 1H)[e]; 4.54 (m/br, 1H)[e] C*H*(CH_3)$_2$: 2.77 (m/br, 1H)[e] N(C*H*$_3$)$_2$: 2.16 (br, 24H)[e] ArC*H*$_3$: 1.46 (s/br, 3H)[e] CH(C*H*$_3$)$_2$: 1.35 (s/br, 3H)[e]; 1.05 (s/br, 3H)[e]	N/A
[$RuCl_2$(*P*,*P*′,*N*,*N*′-mapm)] (**5**)	17.1 (d, $^2J_{PP}$ = 90 Hz, 1P)[e], 8.4 (d, $^2J_{PP}$ = 90 Hz, 1P)[e], 13.7 (s, 2P)[f]	N*H*: 6.61 (q/br, $^3J_{HH}$ = 4.8 Hz, 2H)[f]; 6.01 (q/br, $^3J_{HH}$ = 6.0 Hz, 2H)[f] C*H*$_2$: 4.77 (t, $^2J_{PH}$ = 11.6 Hz, 2H)[f] NC*H*$_3$: 3.06 (d, $^3J_{HH}$ = 6.4 Hz, 6H)[f]; 2.66 (d, $^3J_{HH}$ = 4.8 Hz, 6H)[f]	*C*H$_2$: 55.9 (t, $^1J_{PC}$ = 25 Hz)[f] N*C*H$_3$: 47.8 (s)[f]; 30.6 (s)[f]
[$Ru(CO)_4$(*P*-mapm)] (**6a**)	15.1 (d, $^2J_{PP}$ = 115 Hz, 1P), −66.0 (d, $^2J_{PP}$ = 115 Hz, 1P)	N*H*: 4.65 (q/br, $^3J_{HH}$ = 5.0 Hz, 2H); 4.19 (q/br, $^3J_{HH}$ = 5.0 Hz, 2H) C*H*$_2$: 3.53 (dd, $^2J_{PH}$ = 9.0 Hz, $^2J_{PH}$ = 3.2 Hz, 2H) NC*H*$_3$: 2.74 (d, $^3J_{HH}$ = 5.0 Hz, 6H); 2.54 (d, $^3J_{HH}$ = 5.0 Hz, 6H)	N/A
[$Ru(CO)_3$(*P*,*P*′-mapm)] (**6b**)	−41.3 (s, 2P), −42.0 (s/br 1P)[g], −46.5 (s/br, 1P)[g]	N*H*: 4.95 (q/br, $^3J_{HH}$ = 5.2 Hz, 4H) C*H*$_2$: 4.89 (t, $^2J_{PH}$ = 10.0 Hz, 2H) NC*H*$_3$: 2.59 (d, $^3J_{HH}$ = 5.2 Hz, 12H)	*C*O: 209.4 (t, $^2J_{PC}$ = 13 Hz) *C*H$_2$: 42.0 (t, $^1J_{PC}$ = 27 Hz) N*C*H$_3$: 30.3 (s)
[$Ru_3(CO)_{10}$(μ-*P*,*P*′-mapm)] (**7**)	2.2 (s, 2P)	C*H*$_2$: 4.76 (t, $^2J_{PH}$ = 4.4 Hz, 2H) N*H*: 3.94 (q/br, $^3J_{HH}$ = 2.5 Hz, 4H) NC*H*$_3$: 2.60 (d/br, $^3J_{HH}$ = 2.5 Hz, 12H)	*C*O: 210.9 (s) *C*H$_2$: 45.2 (t, $^1J_{PC}$ = 29 Hz) N*C*H$_3$: 30.5 (s)

[a] NMR abbreviations: s = singlet, d = doublet, t = triplet, q = quartet, sept = septet, br = broad dd = doublet of doublets. All NMR data recorded at 27 °C in CD_2Cl_2 unless otherwise indicated. [b] ^{31}P chemical shifts referenced to external 85% H_3PO_4. [c] ^1H and ^{13}C chemical shifts referenced to external tetramethylsilane. Chemical shifts for aryl groups not given. [d] C_s-symmetric species. [e] C_1-symmetric species. [f] C_2-symmetric species. [g] NMR data at −80 °C.

workup. However, satisfactory elemental analyses and X-ray quality single crystals could not be obtained owing to facile solvent loss.

(b). Dichloro(η^6-*p*-cymene)(diphenyl(*o*-*N*-methylanilinyl)-phosphine)ruthenium(II), [RuCl(η^6-*p*-cymene)(*P*,*N*-Ph_2PAr)]Cl (2b). In a 50 mL three-necked, round-bottom flask with an attached reflux condenser under anhydrous conditions and Ar atmosphere, $[RuCl(\mu\text{-}Cl)(\eta^6\text{-}p\text{-cymene})]_2$ (**1**) (224 mg, 365 μmol) and Ph_2PAr (213 mg, 731 μmol) were stirred in 10 mL of refluxing methanol (at 70 °C) for 2 h over which time the dark red slurry turned to a bright orange solution. The solvent was removed in vacuo, and the viscous residue was dissolved in 5 mL of tetrahydrofuran. After the addition of 15 mL of diethyl ether, a yellow precipitate formed which was then separated from the supernatant by filtration and dried in vacuo producing a yellow powder (380 mg, 87% yield, found: C, 58.09; H, 5.71; N, 2.12. Calcd for $[C_{29}H_{32}Cl_2NPRu]$: C, 58.29; 5.40; 2.34%). Although the crystal structure indicates tetrahydrofuran inclusion, a non-crystalline sample was analyzed here. ^1H NMR analysis in CD_2Cl_2 (obtained at approximately the same time as the elemental analysis) was used to verify solvent content. Single crystals suitable for X-ray crystallographic analysis were obtained by slow evaporation from a 1:1 solution of tetrahydrofuran and diethyl ether. HRMS (ESI): m/z 562.0993 $[M]^+$. Calcd for $C_{29}H_{32}ClNPRu$: m/z 562.0999.

(c). Dichloro(η^6-*p*-cymene)(diphenyl(*o*-*N*-methylanilido)-phosphine)ruthenium(II), [RuCl(η^6-*p*-cymene)(*P*,*N*-Ph_2PAr^-)] (2c). In a 50 mL Schlenk flask under anhydrous conditions and Ar atmosphere, 10 mL of benzene was added to compound **2b** (381 mg, 638 μmol) resulting in yellow slurry. A 10-fold excess of triethylamine (0.89 mL, 6.4 mmol) was added to the slurry while stirring, resulting in an opaque, black-red mixture, to which was then added 10 mL of deoxygenated water. After stirring the mixture for 5 min, the layers were allowed to separate, and the organic layer was transferred to a 50 mL Schlenk tube via cannula under Ar. The solvent and residual triethylamine were removed in vacuo, then 5 mL of tetrahydrofuran was added to the dark residue followed by 30 mL of diethyl ether which resulted in the formation of a precipitate from the dark solution. The solid was collected by filtration, washed with 15 mL of *n*-pentane, and dried in vacuo producing chocolate-colored microcrystals (256 mg, 72% yield, found: C, 61.98; H, 5.60; N, 2.43. Calcd for $[C_{29}H_{31}ClNPRu]$: C, 62.08; H, 5.57; N, 2.50%). Single crystals suitable for X-ray crystallographic analysis were obtained by dissolving the complex, under Ar atmosphere, in a minimum volume of tetrahydrofuran and layering the solution with anhydrous *n*-pentane in a Schlenk tube. HRMS (ESI): m/z 526.1227 $[M - Cl]^+$. Calcd for $C_{29}H_{31}NPRu$: m/z 526.1232.

(d). Dichloro(η^6-*p*-cymene)(diphenyl(*o*-*N*,*N*-dimethylanilinyl)-phosphine)ruthenium(II), [RuCl(η^6-*p*-cymene)(*P*,*N*-Ph_2PAr')]Cl (3b). The orange powder was prepared in a manner similar to that of part (**a**, Method ii) using $[RuCl(\mu\text{-}Cl)(\eta^6\text{-}p\text{-cymene})]_2$ (**1**) (104 mg, 169 μmol) and Ph_2PAr' (104 mg, 339 μmol) and was isolated as an orange powder (200 mg, 96% yield, found: C, 55.37; H, 5.54; N, 2.22. Calcd for $[C_{30}H_{34}Cl_2NPRu]\cdot 2H_2O$: C, 55.64; H, 5.91; N, 2.16%). Although the crystal structure indicates 1 equiv of H_2O and 2 equiv of CH_2Cl_2 per formula unit, a non-crystalline sample was analyzed here which was exposed to air before analysis. ^1H NMR analysis in $CDCl_3$ (obtained at approximately the same time as the elemental analysis) was used to verify water and dichloromethane content. HRMS (ESI) found: m/z 576.1158 for $[M]^+$. Calcd for $[C_{30}H_{34}ClNPRu]$: m/z 576.1155. Single crystals suitable for X-ray crystallographic analysis were obtained by slow evaporation from a saturated dichloromethane solution.

(e). Dichloro(η^6-*p*-cymene)(bis(di(*o*-*N*,*N*-dimethylanilinyl)-phosphino)methane) ruthenium(II), [RuCl(η^6-*p*-cymene)(*P*,*P*′-dmapm)]Cl (4). In a 50 mL Schlenk flask under anhydrous conditions and Ar atmosphere, $[RuCl(\mu\text{-}Cl)(\eta^6\text{-}p\text{-cymene})]_2$ (**1**) (52 mg, 85 μmol) and dmapm (94 mg, 169 μmol) were dissolved in 10 mL of dichloromethane at ambient temperature. The initially red solution was stirred at ambient temperature for 10 min until it had turned orange in color. The solvent volume was reduced to approximately 1 mL in vacuo, and 10 mL of *n*-pentane was added with stirring resulting in an immiscible, red oil which was allowed to settle from the yellow solution. The supernatant was removed via syringe, and the oily residue was dried in vacuo producing an orange powder (115 mg, 79% yield). HRMS (ESI) found: m/z 827.2724 for $[M]^+$. Calcd for $[C_{43}H_{56}ClN_4P_2Ru]$: m/z 827.2707. Single crystals suitable for X-ray crystallographic analysis were obtained by dissolving the complex, under Ar atmosphere, in a minimum volume of CH_2Cl_2 and layering the solution with anhydrous *n*-pentane in an NMR tube.

(f). Dichloro(bis(di(*o*-*N*-methylanilinyl)phosphino)methane)-ruthenium(II), [RuCl$_2$(*P*,*P*′,*N*,*N*′-mapm)] (5). In a 50 mL Schlenk flask under anhydrous conditions and Ar atmosphere, $[RuCl(\mu\text{-}Cl)(\eta^6\text{-}p\text{-cymene})]_2$ (**1**) (105 mg, 194 μmol) and mapm (194 mg, 388 μmol) were cooled to −78 °C (acetone/dry ice bath) and 10 mL of dichloromethane was added. The red-orange slurry was stirred for 5 min before warming to ambient temperature over 15 min. The solvent volume was reduced to approximately 1 mL in vacuo; then 10 mL of *n*-pentane was added to the solution, with stirring, resulting in an orange-yellow precipitate. The solution was filtered under argon, and the solids were washed with 10 mL of *n*-pentane, then dried in vacuo. The solid was dissolved in 5 mL of dichloromethane, and the solution was layered with 15 mL of *n*-pentane and left unstirred for 3 h producing orange-yellow crystals suitable for X-ray crystallographic analysis (282 mg, 95% yield, found: C, 49.78; H, 5.08; N, 7.48%. Calcd for $[C_{29}H_{34}Cl_2N_4P_2Ru]\cdot 0.5CH_2Cl_2$: C, 49.55; H, 4.93; N, 7.84%). HRMS (ESI) found: m/z 637.0985 for $[M - Cl]^+$. Calcd for $[C_{29}H_{34}ClN_4P_2Ru]$: m/z 637.0985.

(g). Tricarbonyl(bis(di(*o*-*N*-methylanilinyl)phosphino)methane)-ruthenium(0), [Ru(CO)$_3$(*P*,*P*′-mapm)] (6b). A 100 mL hexane solution of $[Ru(CO)_4(\eta^2\text{-}C_2H_4)]$ was prepared photolytically with the use of $[Ru_3(CO)_{12}]$ (42 mg, 66 μmol) and an ethylene purge.[31] Under anhydrous conditions and Ar atmosphere, the solution was transferred, via cannula, to a prepared 250 mL Schlenk flask containing mapm (90 mg, 180 μmol). The pale-yellow slurry was stirred for 5 min then 10 mL of dichloromethane was added. The resulting solution was stirred for 2 h, eventually turning orange in color, and was left exposed to ambient light overnight. Solvents were removed in vacuo, and the resulting orange solid was then washed with 10 mL of *n*-pentane. The product was then dried in vacuo and isolated as an orange powder (110 mg, 89% yield, found: C, 55.71; H, 5.12; N, 7.80%. Calcd for $[C_{32}H_{34}N_4O_3P_2Ru]$: C, 56.06; H, 5.00; N, 8.17%). IR (CH_2Cl_2 solution cell): ν_{CO} 2004 (s), 1932 (s) and 1912 (s) cm^{-1}. HRMS (ESI) found: m/z 687.1220 for $[M + H]^+$. Calcd for $[C_{32}H_{35}N_4O_3P_2Ru]$: m/z 687.1222. Single crystals suitable for X-ray crystallographic analysis were obtained by dissolving the complex, under Ar atmosphere, in a minimum volume of CH_2Cl_2 and layering the solution with anhydrous *n*-pentane in an NMR tube.

(h). Decacarbonyl(bis(di(*o*-*N*-methylanilinyl)phosphino)methane)-triruthenium(0,0,0), [Ru$_3$(CO)$_{10}$(*μ*-*P*,*P*′-mapm)] (7). Method i. A 125 mL *n*-pentane solution of $[Ru(CO)_4(\eta^2\text{-}C_2H_4)]$ was prepared photolytically with the use of $[Ru_3(CO)_{12}]$ (48 mg, 75 μmol) and an ethylene purge.[31] Meanwhile, a solution of mapm (52 mg, 104 μmol) in 5 mL of dichloromethane was prepared under Ar atmosphere. In complete darkness, the mapm solution was then transferred to the solution of $[Ru(CO)_4(\eta^2\text{-}C_2H_4)]$ by cannula, and the resulting solution was heated to 50 °C with a water bath while stirring under a brisk flow of Ar to remove the solvents. The red solid residue was then dissolved, in the dark, in 20 mL of dichloromethane and stirred for 5 h under a very slight flow of Ar. The solvent volume was then reduced to approximately 5 mL in vacuo, and 25 mL of *n*-pentane was added resulting in the formation of a yellow precipitate in a bright red solution. The precipitate was allowed to settle, and the red supernatant was removed by cannula. The remaining solid was then dried in vacuo and isolated as an orange-red powder (34 mg, 42% yield,

found: C, 43.86; H, 3.79; N, 4.34%. Calcd for $[C_{39}H_{34}N_4O_{10}P_2Ru_3]\cdot 0.5C_5H_{12}\cdot 0.5CH_2Cl_2$: C, 43.40; H, 3.56; N, 4.82%). IR (CH_2Cl_2 solution cell): ν_{CO} 2079 (m), 2060 (m), 2020 (sh), 2008 (s), 1996 (sh) and 1955 (m) cm^{-1}. Single crystals suitable for X-ray crystallographic analysis were obtained by dissolving the complex, under Ar atmosphere, in a minimum volume of CH_2Cl_2 and layering the solution with anhydrous *n*-pentane in an NMR tube.

Method ii. In a 100 mL Schlenk tube under anhydrous conditions and Ar atmosphere, $[Ru_3(CO)_{12}]$ (133 mg, 208 μmol) and mapm (104 mg, 208 μmol) were dissolved in 25 mL of tetrahydrofuran by stirring the mixture for 10 min at ambient temperature. The initially orange solution was then stirred for 24 h under a very slight flow of Ar, eventually turning bright red in color. The solvent volume was reduced to approximately 5 mL in vacuo, and the solution was then left unstirred and layered with 40 mL of *n*-pentane. After 3 h an orange precipitate had developed, and the supernatant was removed by cannula transfer. The product was then dried in vacuo and isolated as an orange-red powder (151 mg, 67% yield).

X-ray Structure Determinations. (a). General Procedures. Crystals were grown via slow diffusion of *n*-pentane into a benzene (**2a**) or CH_2Cl_2 (**2c**, **3b**, **4**, **5**, **6b**, **7**) solution of the compound, or diffusion of ether into a THF (**2b**) solution of the compound. Data were collected using either a Bruker APEX-II CCD detector/D8 diffractometer[32] with the crystals cooled to −100 °C (**2a**, **2b**, **2c**, **4**, **7**) or a Bruker SMART 1000 CCD detector/PLATFORM diffractometer with the crystals cooled to −80 °C (**3b**, **5**, **6b**); all data were collected using Mo Kα radiation (λ = 0.71073 Å). The data were corrected for absorption through Gaussian integration from indexing of the crystal faces (**2a**, **2b**, **2c**, **3b**, **7**) or through use of a multiscan model (SADABS[32]) (**4**, **5**, **6b**). Structures were solved using Patterson search/structure expansion (DIRDIF-2008[33]) (**2a**), direct methods (SHELXS−97[34]) (**2b**, **2c**, **3b**, **6b**, **7**), or direct methods/structure expansion (SIR97[35]) (**4**, **5**). Refinements were completed using the program SHELXL-97.[34] Hydrogen atoms were assigned positions based on the sp^2 or sp^3 hybridization geometries of their attached carbon or nitrogen atoms, and were given thermal parameters 20% greater than those of their parent atoms. See Supporting Information for a listing of crystallographic experimental data and for selected bond lengths and angles for all structures.

(b). Special Refinement Conditions. (i) **3b**: Distances involving hydrogens of the solvent water molecules were assigned fixed idealized values during refinement (d(O−H) = 0.85 Å; d(H···H) = 1.39 Å). (ii) **5**: The Cl−C distances within the solvent CH_2Cl_2 molecule were restrained to be equal (within 0.03 Å) during refinement. (iii) **7**: Distances within the disordered solvent *n*-pentane and CH_2Cl_2 molecules were subject to the following restraints during refinement: $d(C-C)_{\text{n-pentane}}$ = 1.53(1) Å; $d_{1,3}(C\cdots C)_{\text{n-pentane}}$ = 2.50(1) Å; $d(Cl-C)_{CH_2Cl_2}$ = 1.80(1); $d(Cl\cdots Cl)_{CH_2Cl_2}$ = 2.87(1) Å.

Ketone Transfer Hydrogenation Catalysis. In a 50 mL three-necked, round-bottom flask with an attached reflux condenser under anhydrous conditions and Ar atmosphere, [RuCl(η^6-*p*-cymene)(*P*,*N*-Ph_2PAr^-)] (**2c**, 10.0 mg, 17.8 μmol) was dissolved in isopropanol (*i*-PrOH, 13.6 mL, 178 mmol). The mixture was heated to 90 °C for 1.0 min while stirring which resulted in an orange-brown solution. Acetophenone (2.08 mL, 17.8 mmol) was then added to the refluxing mixture followed immediately by solid potassium *tert*-butoxide (*t*-BuOK, 8.0 mg, 71 μmol), which was added to the reaction flask under a light stream of Ar (t_{rxn} = 0 min) and resulted in darkening to a red-brown solution. The molar composition of the reaction mixture at this point was [Ru]: *t*-BuOK: acetophenone: *i*-PrOH = 1:4:1,000:10,000. Aliquots were withdrawn at t_{rxn} = 0, 5, 60, and 120 min which were immediately filtered through columns containing 2 cm of acidic alumina atop 2 cm of Florisil (to remove catalyst) and collected in vials which were quickly capped. Each sample was analyzed by ^{1}H NMR analysis ($CDCl_3$) within 10 min of its withdrawal from the reaction mixture. GC-EI-MS analysis was carried out on the filtered samples after 10-fold volumetric dilution with dichloromethane. Conversion percentages, turnover numbers, and frequencies determined from acetophenone and 1-phenylethanol signals in both ^{1}H NMR and GC-EI-MS analyses were mutually consistent.

Scheme 1

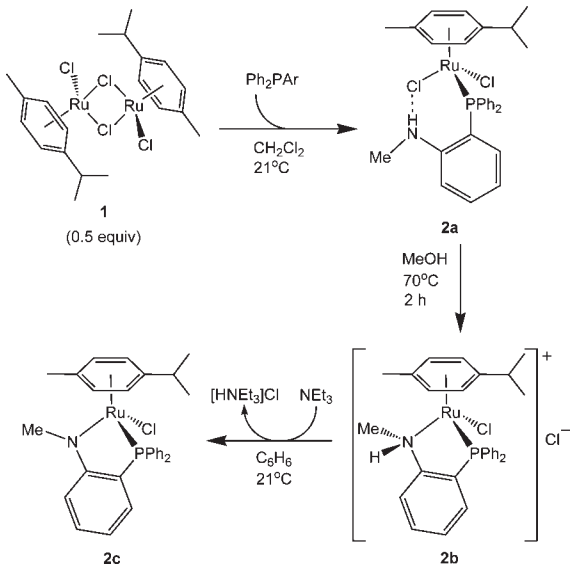

Results and Discussion

(a). Monophosphinoaniline Complexes. (i). Diphenyl(*o*-*N*-methylanilinyl)phosphine. The monophosphinoaniline ligand, Ph_2PAr (Ar = *o*-C_6H_4NHMe) reacts with 0.5 equiv of [RuCl(μ-Cl)(η^6-*p*-cymene)]$_2$ (**1**), under mild conditions in dichloromethane to produce the neutral complex, [$RuCl_2$(η^6-*p*-cymene)(*P*-Ph_2PAr)] (**2a**), in which the chloro-bridged dimer has been cleaved by coordination of the phosphine donor while the amine functionality remains uncoordinated and pendent (Scheme 1). The $^{31}P\{^1H\}$ NMR spectrum of **2a** displays the expected singlet at δ_P 28.2 while the ^{1}H NMR spectrum shows a doublet at δ_H 2.81, representing the NMe protons having $^3J_{HH}$ = 5.0 Hz because of coupling with the amine hydrogen (δ_H 5.47, q/br). The phosphorus chemical shift of **2a** is similar to that of the non-*N*-methylated analogue, [$RuCl_2$(η^6-*p*-cymene)(*P*-$Ph_2PC_6H_4NH_2$)] (δ 28.9), reported by Pelagatti et al.[16] Moreover, the *N*-methyl signal of **2a** has a chemical shift similar to that of the free Ph_2PAr ligand (δ_H 2.84) suggesting that the amine is not coordinated. The methyl protons of the isopropyl group of **2a** are all represented by a doublet at δ_H 1.39, displaying vicinal coupling with the adjacent methine proton ($^3J_{HH}$ = 7.0 Hz). The $^{13}C\{^1H\}$ NMR spectrum of **2a** shows signals for the aliphatic carbons, which were identified between

(32) Programs for diffractometer operation, unit cell indexing, data collection, data reduction, and absorption correction were those supplied by Bruker.

(33) Beurskens, P. T.; Beurskens, G.; de Gelder, R.; Smits, J. M. M; Garcia-Granda, S.; Gould, R. O. *DIRDIF-2008 program system*; Crystallography Laboratory, Radboud University : Nijmegen, The Netherlands, 2008.

(34) Sheldrick, G. M. *Acta Crystallogr.* **2008**, *A64*, 112–122.

(35) Altomare, A.; Burla, M. C.; Camalli, M.; Cascarano, G. L.; Giacovazzo, C.; Guagliardi, A.; Moliterni, A. G. G.; Polidori, G.; Spagna, R. *J. Appl. Crystallogr.* **1999**, *32*, 115–119.

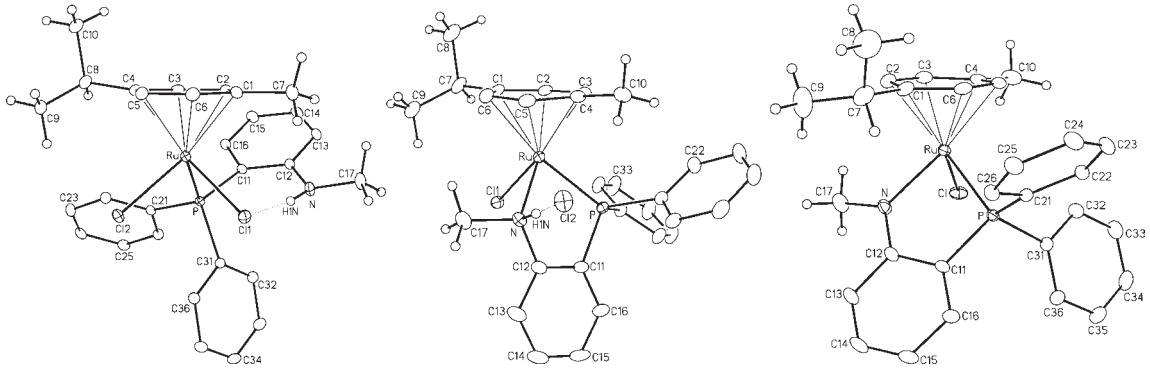

Figure 1. ORTEP diagrams showing [$RuCl_2(\eta^6$-*p*-cymene)(*P*-Ph_2PAr)] (**2a**, left), [$RuCl(\eta^6$-*p*-cymene)(*P*,*N*-Ph_2PAr)]Cl (**2b**, center), and [$RuCl(\eta^6$-*p*-cymene)(*P*,*N*-Ph_2PAr^-)] (**2c**, right). Gaussian ellipsoids for all non-hydrogen atoms are depicted at the 20% probability level. Hydrogen atoms, where included, are shown artificially small.

δ_C 30.9 and 18.1 by gradient heteronuclear single quantum coherence (GHSQC) analysis.

The solid state structure of complex **2a** (Figure 1, left) displays a hydrogen bond between one of the inner-sphere chlorides and the pendent amine hydrogen, for which the resulting H(N1)−Cl(1) distance of 2.43 Å is significantly shorter than a normal van der Waals separation of 3.05 Å.[36] An analysis of the structural parameters within complex **2a** reveals that the Ru−Cl(1) bond is slightly longer than Ru−Cl(2) (2.4258(4) vs 2.4035(3) Å) presumably because of its interaction with the pendent amine hydrogen. The previously reported structure of the non-*N*-methylated analogue of **2a**, [$RuCl_2(\eta^6$-*p*-cymene)-(*P*-$Ph_2P(o$-$C_6H_4NH_2)$)], also shows a similar hydrogen bond.[16]

Interestingly, while the *N*-methyl, methine, and arylmethyl carbon resonances of **2a** appear as sharp singlets, the signals for the methyl carbons of the isopropyl group (δ_C 22.0), as well as some aromatic carbon signals, are broad. Such broadening suggests fluxionality that we propose results from the intramolecular hydrogen bond involving the amine hydrogen and a chloro ligand being weak enough to allow for facile enantiomerization via movement from one chloro ligand to the other, yet strong enough to render some carbon environments pseudodiastereotopic on the NMR time scale. A $^{13}C\{^1H\}$ NMR spectroscopic analysis carried out at −80 °C supports this hypothesis as two sharp signals representing the isopropyl methyl carbons are now observed at this temperature at δ_C 24.3 and 19.6. The molar conductivity of **2a** is Λ = 6 $cm^2\ \Omega^{-1}\ mol^{-1}$, consistent with a non-conducting complex.

While **2a** is indefinitely stable in dichloromethane solution, the compound can be converted to the cationic *P*,*N*-chelated isomer, [$RuCl(\eta^6$-*p*-cymene)(*P*,*N*-Ph_2PAr)]Cl (**2b**) in refluxing methanol within hours (Scheme 1). Faraone et al. have shown that protic solvents kinetically enhance amine coordination in a similar complex by providing strong hydrogen bond donors to facilitate the dissociation of a chloro ligand.[37] Although the solid-state structure of **2a** (vide supra) clearly depicts a hydrogen bond between the pendent amine hydrogen and a chloro ligand, it appears that, rather than promoting chloride ion dissociation, this intramolecular hydrogen bond actually appears to stabilize the monodentate complex against chelation of the amine by orienting the lone pair on nitrogen away from the metal. Once formed, the chelate complex **2b** is never observed to revert back to **2a**. Chelation in **2b** results in a significant downfield shift of the ^{31}P resonance to δ_P 53.4 because of the effect of the five-membered ring[38] as also reported for the non-*N*-methylated analogue.[16] The ^1H NMR spectrum shows a broad signal at δ_H 10.8 representing the deshielded amine hydrogen which becomes quite acidic upon coordination of the amine to the cationic ruthenium center; the doublet *N*-methyl proton resonance found at δ_H 3.52 (with $^3J_{HH}$ = 4.4 Hz) is also shifted downfield from that of **2a**. The chirality of **2b** is made evident by two distinct signals representing diastereotopic methyl groups of the isopropyl moiety at δ_H 1.33 and 1.31 each of which appears as a doublet because of vicinal coupling ($^3J_{HH}$ = 7.0 Hz) with the methine hydrogen. The $^{13}C\{^1H\}$ NMR spectrum of **2b** shows a strongly deshielded *N*-methyl carbon resonance at δ_C 76.7 because of its geminal relationship to the formally cationic ruthenium center. The molar conductivity of **2b** is Λ = 59 $cm^2\ \Omega^{-1}\ mol^{-1}$, consistent with a 1:1 electrolyte.

The X-ray structure of **2b** (Figure 1, middle) shows a strong hydrogen bond between the outer-sphere chloride anion (Cl(2)) and the coordinated amine hydrogen (H(1N); 2.16 Å), which is consistent with the extensive deshielding of this proton observed spectroscopically, while also clearly illustrating the diastereotopicity of the isopropyl methyl groups of the *p*-cymene ligand, consistent with the observation of two distinct signals for these groups in both the ^1H and $^{13}C\{^1H\}$ NMR spectra.

The acidic amine hydrogen of **2b** is readily deprotonated to give the corresponding amido complex, [$RuCl(\eta^6$-*p*-cymene)(*P*,*N*-Ph_2PAr^-)] (**2c**, Ar^- = *o*-$C_6H_4NMe^-$; Scheme 1). Addition of 10 equiv of triethylamine to a slurry of **2b** in benzene resulted in immediate darkening to an opaque, black-red mixture from which the triethylammonium chloride byproduct was easily removed by aqueous extraction, yielding **2c** as a brown, microcrystalline solid. Spectroscopic analysis of **2c** shows the phosphorus resonance at δ_P 59.3, which is shifted even further downfield from that of **2b**. Interestingly, the ^1H NMR spectrum of **2c** in CD_2Cl_2 shows broad signals at ambient temperature and, notably, the proton signals for the two diastereotopic isopropyl methyl groups of the *p*-cymene unit

(36) Zefirov, Y. V.; Zorkii, P. M. *Russ. Chem. Rev.* **1989**, *58*, 421–440.
(37) Arena, C. G.; Calamia, S.; Faraone, F.; Graiff, C.; Tiripicchio, A. *J. Chem. Soc., Dalton Trans.* **2000**, 3149–3157.
(38) Garrou, P. E. *Chem. Rev.* **1981**, *81*, 229.

Scheme 2. Enantiomerization of **2c** via Coordinatively Unsaturated Intermediate **2d**

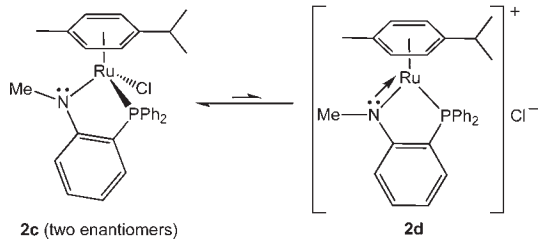

2c (two enantiomers) **2d**

coalesce at 40 °C. Such fluxional behavior implies that a rapid enantiomerization process is occurring in solution, presumably by chloride ion dissociation to generate the cationic, coordinatively unsaturated intermediate, [Ru(η^6-*p*-cymene)(*P*,*N*-Ph_2PAr^-)]Cl (**2d**, Scheme 2), followed by recoordination of the chloride ion on the opposite face of the chelate ring, resulting in stereoinversion at ruthenium. A fluxional process involving stereoinversion at nitrogen seems less likely since such a mechanism would involve two diastereoisomers which should produce two signals in the $^{31}P\{^1H\}$ NMR spectrum. Futhermore, the X-ray structure of **2c**, discussed below, reveals nearly perfect planarity of the amido nitrogen, suggesting that lone pair inversion is not a likely cause for the observed fluxionality. The conductivity of complex **2c** was found to be $\Lambda = 23\ cm^2\ \Omega^{-1}\ mol^{-1}$, which is intermediate between that of a neutral species and a 1:1 electrolyte, supporting the equilibrium shown in Scheme 2. Pellagatti reports a computationally determined energy difference between two species, that are structurally analogous to **2c** and **2d**, of only $\Delta G = 2.9$ kcal/mol, with the cationic, coordinatively unsaturated complex (similar to **2d**) being less stable.[16] Our variable temperature NMR analysis of **2c** indicates that its enantiomerization, at the coalescence temperature of the proton signals for the methyl groups of the isopropyl moiety ($T_{coal} = 40$ °C), occurs with a rate constant of $k_{coal} = 95\ s^{-1}$, corresponding to an energy barrier of $\Delta G^{\ddagger}$ (313 K) = 15 kcal/mol.[39]

A representation of the amido complex **2c** is shown in Figure 1 (right), confirming the spectroscopic characterization of this species. The three structures depicted in Figure 1 clearly illustrate the transition of the complex with the Ph_2PAr ligand in a monodentate, *P*-bound coordination mode (**2a**), to the *P*,*N*-chelate (**2b**), to the amido species (**2c**). The η^6-*p*-cymene unit appears normal in all of the monophosphinoaniline complexes with relatively small deviations in Ru−C_{arene} bond lengths. Compound **2c** has a significantly shorter Ru−N bond length (2.086(2) Å) than that of **2b** (2.172(2) Å) owing presumably to both the decreased steric demand of the deprotonated donor and the greater basicity of the formally anionic amido nitrogen in **2c** which strengthens the Ru−N bond. The three atoms bound to the amido nitrogen atom of **2c** (Ru, C(17), C(12)) are arranged in an approximate trigonal plane as is evident from the sum of the three angles about nitrogen (358.0°) and can be compared to the sum of the same three angles (341.0°) in **2b** containing the pyramidal nitrogen. The planarity of the amido group illustrates the strong sp^2 character of the nitrogen atom suggesting some degree of π-donation to ruthenium which could also be reflected in the short Ru−N bond (vide supra).

(ii). Diphenyl(*o*-*N*,*N*-dimethylanilinyl)phosphine. Pelagatti et al. have reported that reaction of the *N*,*N*-dimethyl analogue, Ph_2PAr', with 0.5 equiv of **1** initially results in the pendent, monodentate complex, [$RuCl_2$(η^6-*p*-cymene)-(*P*-Ph_2PAr')] (**3a**) analogous to **2a**, which over time in dichloromethane converted to the *P*,*N*-chelated species, [RuCl(η^6-*p*-cymene)(*P*,*N*-Ph_2PAr')]Cl (**3b**),[16] in which the amine has replaced a chloro ligand at ruthenium to generate a cationic complex analogous to **2b** (see Scheme 3). In our hands, however, the intermediate **3a** was never observed. Despite our best efforts to exclude moisture from reaction mixtures, the hygroscopic intermediate **3a** readily sequesters adventitious water, as is observed by ^1H NMR spectroscopy, elemental analysis, and X-ray crystallography of **3b** (which showed the presence of water in the unit cell), which appears to facilitate chelation by hydrogen-bonding assisted chloride ion abstraction.[16,37] Unfortunately very little characterization of the intermediate **3a** is given in the report of this compound beyond the $^{31}P\{^1H\}$ NMR chemical shift; the other spectroscopic data given for this compound[16] appear to be those of **3b**, as shown by comparison with our data. The apparent ease with which intermediate **3a** is able to undergo chelation under mild conditions contrasts the protic, forcing conditions necessary to promote chelation in **2a**. Presumably, the intramolecular hydrogen bond between the amine hydrogen and a chloro ligand in **2a** (Figure 1) renders the pendent amine more inert to chelation (vide supra), while the more nucleophilic *N*,*N*-dimethylanilinyl group of **3a** rapidly displaces a chloro ligand to generate the cationic, chelated product, **3b**.[37] Coordination of the *N*,*N*-dimethylanilinyl group is favored despite the increased steric bulk of this group compared with the *N*-methyl analogue.

The $^{31}P\{^1H\}$ NMR spectrum of **3b** shows a singlet at δ_P 47.5 (CD_2Cl_2) which is shifted significantly downfield from those of **2a** or **3a**[16] and is again consistent with the presence of a five-membered chelate ring.[38] The *P*,*N*-chelation mode of **3b** is demonstrated by ^1H NMR spectroscopy which shows two distinct, relatively downfield singlets (δ_H 4.04 and 3.50) for the diastereotopic *N*-methyl groups, a result of the stereogenic center created at ruthenium upon coordination of the amine. The asymmetry of **3b** is also made evident by two distinct doublet resonances for the methyl protons of the *p*-cymene isopropyl group (δ_H 1.26 and 1.35, $^3J_{HH} = 7.0$ Hz), as well as four chemically distinct aromatic *p*-cymene proton signals between δ_H 7.32 and 5.18, which were identified by gradient correlation spectroscopic (GCOSY) analysis. By contrast with **2a**, the $^{13}C\{^1H\}$ NMR spectrum of **3b** shows two sharp singlets for the methyl carbons of the isopropyl groups at δ_C 22.3 and 20.7 and relatively deshielded *N*-methyl resonances at δ_C 65.2 and 58.4, consistent with amine coordination to a formally cationic ruthenium center. The molar conductivity of **3b** is $\Lambda = 79\ cm^2\ \Omega^{-1}\ mol^{-1}$, characteristic of a 1:1 electrolyte. The *p*-cymene ligands of the monophosphinoaniline complexes remain coordinated and are not displaced, even in the presence of an excess of the ligands Ph_2PAr and Ph_2PAr', respectively. This presumably reflects the strong binding affinity of the η^6-*p*-cymene ligand and is apparently not the result of any inherent instability of the presumed products,

(39) Bain, A. D. *Prog. Nucl. Magn. Reson. Spectrosc.* **2003**, *43*, 63–103.

Scheme 3

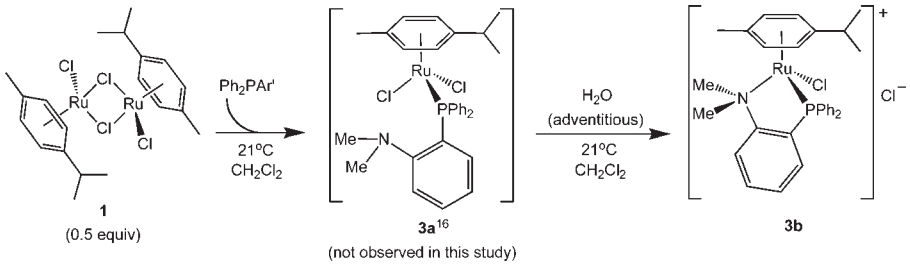

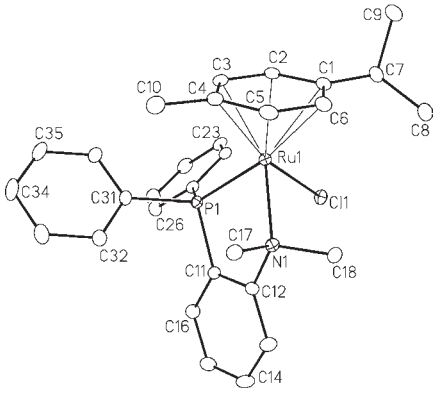

Figure 2. ORTEP diagram of one of two crystallographically independent molecules of [RuCl(η^6-*p*-cymene)(*P*,*N*-Ph_2PAr')]$^+$ (cation of **3b**). Gaussian ellipsoids for all non-hydrogen atoms are depicted at the 20% probability level. Hydrogen atoms are not shown.

[$RuCl_2$(*P*,*N*-Ph_2PAr)$_2$] and [$RuCl_2$(*P*,*N*-Ph_2PAr')$_2$], since a number of analogous species are known.[8,11,40,41]

The X-ray structural analysis of **3b** shows the Ru−Cl bond lengths of 2.3944(6) and 2.3982(6) Å which are close to that of **2b** (2.3947(6) Å) and the non-hydrogen-bonded chloro ligand in **2a** (2.4035(3) Å) (Figure 2). The Ru−P bond lengths in the chelated complexes **2b**, **2c**, and **3b** (each ∼2.30 Å) are shorter than that of the pendent complex **2a** (∼2.36 Å) presumably because of the constraints imposed by the chelate rings. The crystal structure of **3b** clearly shows the chemically distinct *N*-methyl groups of the coordinated amine. A comparison of the Ru−N bond lengths in structural analogues **2b** and **3b** illustrates the steric effects of the additional *N*-methyl group on the length of the Ru−N bond as that of **2b** (2.172(2) Å) is shorter than that of **3b** (2.199(2) and 2.209(2) Å for the two independent molecules) despite the stronger σ-donor character of the *N*,*N*-dimethylanilinyl donor.

(iii). Ketone Transfer Hydrogenation Catalysis. Compounds **2c** and **2d** are of interest since similar species were recently proposed as intermediates involved in efficient ketone transfer hydrogenation catalysis, likely operating by a mechanism involving the simultaneous transfer of protic and hydridic hydrogen atoms from reagent alcohol to the coordinatively unsaturated amido complex (similar to **2d**) via an outer-sphere mechanism.[16] Herein we have verified that the amido species (**2c**) under basic conditions is also an efficient catalyst for the transfer hydrogenation of acetophenone from isopropanol to produce 1-phenylethanol and acetone. Although this reaction has already been studied using the *N*,*N*-dimethyl complex, **3b**, as well as the non-*N*-methylated analogue, [RuCl(η^6-*p*-cymene)(*P*,*N*-Ph_2P(*o*-$C_6H_4NH_2$))]Cl (**2e**), as catalysts,[16] we sought to compare the catalytic activity of the *N*-methylamido compound, **2c**, with those previously reported. Not surprisingly perhaps, under similar conditions the *N*-methylamido complex, **2c**, exhibits a catalytic activity intermediate between the more active non-*N*-methylated complex, **2e**, and the less active *N*,*N*-dimethyl complex, **3b**[16] (Table 2).

In principle, compound **2c** could function as a transfer hydrogenation catalyst in the absence of base, via the Noyori bifunctional mechanism[23,24] whereby the amido species is converted into the catalytically active amine-hydride by H^+/H^- transfer from isopropanol. However, Entry 7 shows that **2c** is inactive as a catalyst in the absence of base. This suggests that an amido-hydride species, generated from **2c** via chloride replacement by isopropoxide followed by β-hydride elimination, may be the catalytically active species. However, this possibility remains to be tested. It should also be noted that a related NMe_2-containing complex, which cannot function by the bifunctional mechanism, has also been shown to require base, yet the derived hydride species was found to be inactive as a catalyst.[26] Another possible mechanism that needs to be investigated is the Meerwein−Ponndorf−Verley−Oppenauer mechanism in which simultaneous coordination of both the alkoxide and the ketone to the metal leads to direct transfer of the β-hydrogen on the alkoxide to the ketone without the formation of a hydrido complex.[23,42,43]

The *N*,*N*-dimethyl complex (**3b**) is believed to operate by an inner-sphere mechanism[16] since amine deprotonation to afford an amido species is not possible and hemilability of the Ph_2PAr' ligand (via displacement of the amine from ruthenium) seems more likely.[22] Although the amine complex, **2b**, itself was never tested as a transfer hydrogenation catalyst, it can be assumed that the addition of *t*-BuOK to reaction mixtures would immediately deprotonate **2b** to give the amido complex, **2c**, since even weakly basic triethylamine instantly deprotonates **2b**. With amido complex **2c** in hand, we are currently attempting to isolate the hydrido-amine complex,

(40) Jia, W.; Chen, X.; Guo, R.; Sui-Seng, C.; Amoroso, D.; Lough, A. J.; Abdur-Rashid, K. *Dalton Trans.* **2009**, 8301–8307.
(41) Rauchfuss, T. B.; Patino, F. T.; Roundhill, M. *Inorg. Chem.* **1975**, *14*, 652–656.
(42) Vinzi, F.; Zassinovich, G.; Mestroni, G. *J. Mol. Catal.* **1983**, *18*, 359–366.
(43) (a) Meerwein, H.; Schmidt, R. *Justus Liebigs Ann. Chem.* **1925**, *444*, 221. (b) Ponndorf, W. *Z. Angew. Chem.* **1926**, *39*, 138. (c) Verley, A. *Bull. Chem. Soc. Chim. Fr.* **1925**, *37*, 537. (d) Oppenauer, R. V. *Recl. Trav. Chim. Pays-Bas* **1937**, *56*, 137. (e) Wilds, A. L. *Org. React.* **1944**, *2*, 178. (f) Djerassi, C. *Org. React.* **1951**, *6*, 207.

Table 2. Effects of *N*-methyl Substitution on Acetophenone Transfer Hydrogenation Activities

entry	complex	no. of *N*-Me groups	t_{rxn} (min)	conversion (%) [a]	TOF (h^{-1}) [b]
1[16]	**2e**[c]	0	5	37	4440
2[16]	**2e**[c]	0	60	≥98	≥980
3[16]	**2e**[d]	0	60		
4	**2c**[e]	1	5	13	1560
5	**2c**[e]	1	60	34	340
6	**2c**[e]	1	120	46	230
7	**2c**[d]	1	60		
8[16]	**3b**[c]	2	60	10	100

[a] Determined by CG analysis. [b] Turnover frequency determined at the corresponding reaction time (t_{rxn}) in column 4. [c] Reaction conditions: Temperature = 90 °C; Ru/KOH/acetophenone/*i*-PrOH = 1:4:1,000:128,000. [d] In the absence of base. [e] Reaction conditions: Temperature = 90 °C; Ru/*t*-BuOK/acetophenone/*i*-PrOH = 1:4:1,000:10,000.

$[RuH(\eta^6\text{-}p\text{-cymene})(P,N\text{-}Ph_2PAr)]^+$, as well as the hydrido-amido complex, $[RuH(\eta^6\text{-}p\text{-cymene})(P,N\text{-}Ph_2PAr^-)]$, to test these species as ketone transfer hydrogenation catalysts.

(b). Diphosphinoaniline Complexes. In addition to the monophosphinoanilines we were also interested in the analogous diphosphines, $Ar_2PCH_2PAr_2$ (Ar = *o*-C_6H_4NHMe; mapm) and $Ar'_2PCH_2PAr'_2$ (Ar′ = *o*-$C_6H_4NMe_2$; dmapm), and the effects of *N*-methyl substitution on the coordination modes displayed by these ligands. Reaction of dmapm with 0.5 equiv of $[RuCl(\mu\text{-}Cl)(\eta^6\text{-}p\text{-cymene})]_2$ (**1**), shown in Scheme 4, occurs much as observed earlier for the Ph_2PAr' ligand, in which an inner-sphere chloride is lost to allow dmapm to bind as a bidentate ligand, while the *p*-cymene ligand remains bound to Ru. However, the product observed in the solid state, $[RuCl(\eta^6\text{-}p\text{-cymene})(P,P'\text{-dmapm})]Cl$ (**4**), differs from **3** by displaying *P*,*P*′-chelation rather than the *P*,*N*-coordination mode observed in the monophosphine analogue.

Surprisingly, the $^{31}P\{^1H\}$ NMR spectrum of **4** actually shows two species in solution. The expected sharp singlet of **4**, at δ_P −1.5, which is consistent with the structure shown for **4** in Scheme 4, and as determined in the X-ray structure analysis (vide infra), is in fact the minor species, while a species displaying two broad doublets, at δ_P 1.5 and −15.4 ($^2J_{PP}$ = 56 Hz), predominates in a 6:1 ratio. By comparison, the $^{31}P\{^1H\}$ NMR spectrum of the closely related dppm analogue displays only the expected singlet at δ_P 2.7 (in $CDCl_3$).[44] The mass spectrum of **4** shows only one predominant signal pattern consistent with that calculated for the formulation of the cation depicted in Scheme 4, supporting our hypothesis that the non-symmetrical species is an isomer of the symmetrical *P*,*P*′-chelate observed in the solid state.

A $^{31}P\{^1H\}$ spin saturation transfer (SST) experiment was carried out on a sample of **4** in CD_3NO_2 at 40 °C by irradiating the resonance at δ_P −15.4, resulting in a significant reduction in the intensity of the signals at δ_P 1.5 and −1.5 relative to an internal standard, indicating that all three phosphorus environments are undergoing chemical exchange at this temperature. We have considered a couple of structures that could give rise to an unsymmetrical species having two ^{31}P environments but neither seems possible. We have ruled out the possibility

Scheme 4. Syntheses of Diphosphinoaniline Complexes of Ruthenium

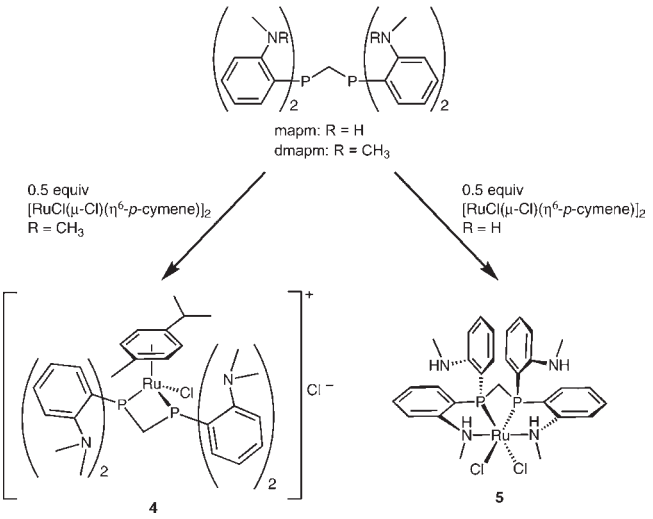

that coordination of an anilinyl nitrogen could displace the other end of the diphosphine, to give a *P*,*N*-chelated species like **3b**, on the basis that neither ^{31}P resonance has a chemical shift consistent with free dmapm (δ_P −36.0)[30] or the pendent phosphines of other reported dmapm complexes (δ_P −41.3 and −41.8).[45] In addition, the molar conductivity of Λ = 62 $cm^2\ \Omega^{-1}\ mol^{-1}$, which is consistent with a 1:1 electrolyte in nitromethane, is inconsistent with dmapm functioning as a tridentate ligand in a *P*,*P*′,*N*-chelation mode, through displacement of the second chloro ligand.

The fluxionality of complex **4** is made evident by the SST experiment and by the broad signals in both the ^1H and the $^{31}P\{^1H\}$ NMR spectra which exhibit temperature dependent chemical shifts and line-shapes. Variable temperature $^{31}P\{^1H\}$ NMR spectroscopic analysis of **4** shows that the 6:1 ratio of the non-symmetric complex to the C_s-symmetric *P*,*P*′-chelate between −80 and 50 °C remains relatively unchanged (even after replacing CD_2Cl_2 solvent with CD_3NO_2), although all signals sharpen upon cooling. Furthermore, between 50 and 80 °C, the signal belonging to the C_s-symmetric isomer is coincidentally overlapping with the more downfield signal of the non-symmetrical species. Unfortunately, the variable temperature ^1H NMR analysis is not useful as a means of characterization for compound **4** because of very broad, overlapping aromatic and *N*-methyl signals over the entire temperature range studied (−80 to 80 °C), rendering the identity of the major solution isomer unknown.

The solid state structure of **4** (Figure 3) also fails to provide clues about the nature of the non-symmetrical solution species, showing that the isopropyl unit of the *p*-cymene fragment should not be restricted from freely rotating about the isopropyl-aryl and ruthenium-arene bond axes, suggesting that this particular geometry should possess chemically equivalent phosphorus nuclei. However, dissolution of the crystalline sample in CD_2Cl_2 and subsequent $^{31}P\{^1H\}$ NMR spectroscopic analysis shows the same 6:1 concentration ratio of C_1- to C_s-symmetric isomers as discussed above. The Ru−Cl bond length in **4**

(44) Jensen, S. B.; Rodger, S. J.; Spicer, M. D. *J. Organomet. Chem.* **1998**, *556*, 151–158.

(45) Dennett, J. N. L.; Bierenstiel, M.; Ferguson, M. J.; McDonald, R.; Cowie, M. *Inorg. Chem.* **2006**, *45*, 3705–3717.

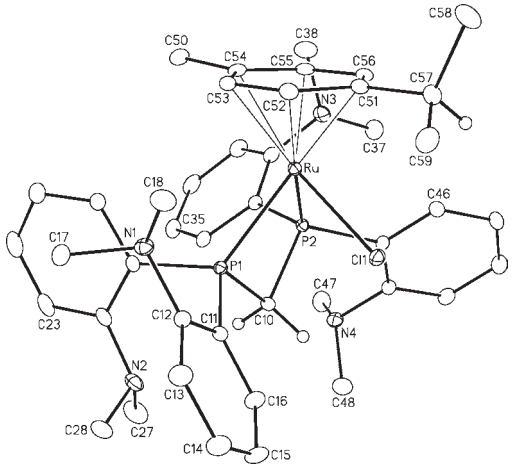

Figure 3. ORTEP diagram of one of two crystallographically independent cations of [RuCl(η^6-*p*-cymene)(*P*,*P*′-dmapm)]Cl (**4**). Thermal ellipsoids as in Figure 1.

(2.3938(6) and 2.3928(6) Å for the two independent molecules) is similar to that of **3b** (2.3944(6) and 2.3982(6) Å). However, complex **4** has slightly greater Ru−P bond lengths (between 2.3851(7) and 2.3313(6) Å) than that of **3b** (2.3059(7) and 2.3005(7) Å), presumably because of the greater strain of the four-membered chelate ring in addition to the increased steric congestion at Ru in **4**. Interestingly, the chelate ring of **4** is quite puckered with Ru−P(1)−C(10)−P(2) and Ru−P(2)−C(10)−P(1) torsional angles for the two independent molecules between 18.5(1)° and 22.99(9)° as the methylene unit is bent slightly out of the plane of the ring toward the chloro ligand.

Although the monophosphinoaniline complexes discussed (vide supra) exhibit different coordination tendencies depending on the degree of methyl substitution at the amine, diverse coordination behavior at ruthenium is even more pronounced when comparing the diphosphinoanilines (mapm vs dmapm). Unlike the reaction described above for dmapm, reaction of mapm with 0.5 equiv of **1** at ambient temperature in dichloromethane results in facile displacement of the *p*-cymene moiety to generate the tetradentate complex, [$RuCl_2$(*P*,*P*′,*N*,*N*′-mapm)] (**5**, Scheme 4). Both complexes **4** and **5** were synthesized in dichloromethane solution followed by washing with *n*-pentane (to remove any *p*-cymene that may have been produced) and were isolated as orange powders in good yields. Upon exposure to water or prolonged exposure to air, samples of both **4** and **5** turn green, presumably because of oxidative decomposition[46] to yet unidentified species. Although exposure of **5** to water or other protic solvents could promote chloride ion displacement and concomitant coordination of an additional amine to generate a cationic complex, we have not yet investigated this reaction. The formation of such a pentadentate complex could produce numerous stereoisomers which should be expected to complicate spectroscopic analysis.

The ^{1}H spectrum of **5** is complicated since the complex is formed as a mixture of stereoisomers. Single crystal X-ray structural analysis of **5**·0.5CH_2Cl_2 shows

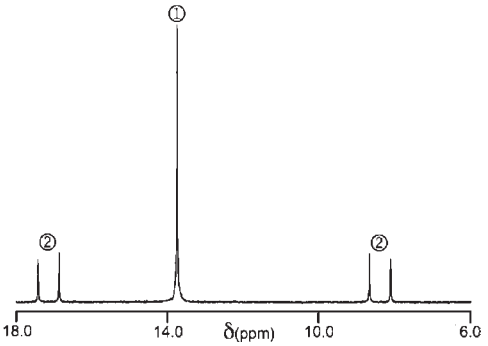

Figure 4. $^{31}P\{^1H\}$ NMR spectrum of **5** in CD_2Cl_2. Signal ① corresponds to C_2-symmetric stereoisomers; signals ② correspond to C_1-symmetric stereoisomers.

disorder in one of the coordinated *N*-methylamino groups over two diastereotopic positions with a 60:40 site occupancy ratio representing C_2- and C_1-symmetric stereoisomers, respectively. Dissolution of the crystalline sample in CD_2Cl_2 and subsequent NMR spectroscopic analyses also indicate the presence of these stereoisomers in a ratio similar to that observed in the solid state, confirming that these isomers co-crystallize. The $^{31}P\{^1H\}$ NMR spectrum of **5** (Figure 4) shows a prominent singlet at δ_P 13.7, attributed to the P_R,P'_R,N_R,N'_R configuration (ORTEP shown later) and its corresponding enantiomer. In this configuration, the phosphorus nuclei are equivalent by a C_2-symmetry axis. In addition to this signal are two doublets at δ_P 17.1 and 8.4 ($^2J_{PP}$ = 90 Hz), attributed to the P_R,P'_R,N_S,N'_R configuration and its corresponding enantiomer. The integrated signal intensities show that the ratio of these C_2- to C_1-symmetric stereoisomers is approximately 3:2 (mol/mol) and that there is no evidence of the other possible C_1- and C_2-symmetric stereoisomers.

The ^{1}H NMR spectrum of the C_2-symmetric configurations of **5** shows two doublets at δ_H 3.06 ($^3J_{HH}$ = 6.0 Hz) and at 2.66 ($^3J_{HH}$ = 4.8 Hz) representing the pendent and coordinated *N*-methyl protons, respectively. These signals exhibit vicinal coupling to the amine hydrogens which resonate at δ_H 6.01 and 6.61, respectively, and appear as broad quartets. The methylene protons of the diphosphine backbone produce a triplet resonance at δ_H 4.78 with $^2J_{PH}$ = 11.6 Hz, confirming the chemical equivalence of the neighboring phosphines. The $^{13}C\{^1H\}$ NMR spectrum of **5** shows a triplet at δ_C 55.9 ($^1J_{PC}$ = 25 Hz) for the methylene carbon and two singlet resonances at δ_C 47.8 and 30.6 belonging to coordinated and pendent *N*-methylamino groups, respectively. The ambient temperature spectroscopic observation of two well-defined *N*-methyl environments within this C_2-symmetric isomer shows no evidence for Type II hemilability,[1] whereby the pendent anilines could, in principle, reversibly displace the coordinated ones, resulting in coalescence of the *N*-methyl proton signals. The lack of such inherent fluxionality at ruthenium(II) is in contrast to a similar series of rhodium(I) complexes which were shown to display Type II hemilability by ^{1}H NMR spectroscopy.[22] The molar conductivity of **5** was found to be Λ = 7 cm^2 Ω^{-1} mol^{-1}, consistent with a non-conducting complex.

X-ray structural analysis of compound **5** reveals a centrosymmetric unit cell with a disordered *N*-methyl

(46) Murray, K. S.; van den Bergen, A. M.; West, B. O. *Aust. J. Chem.* **1978**, *31*, 203–207.

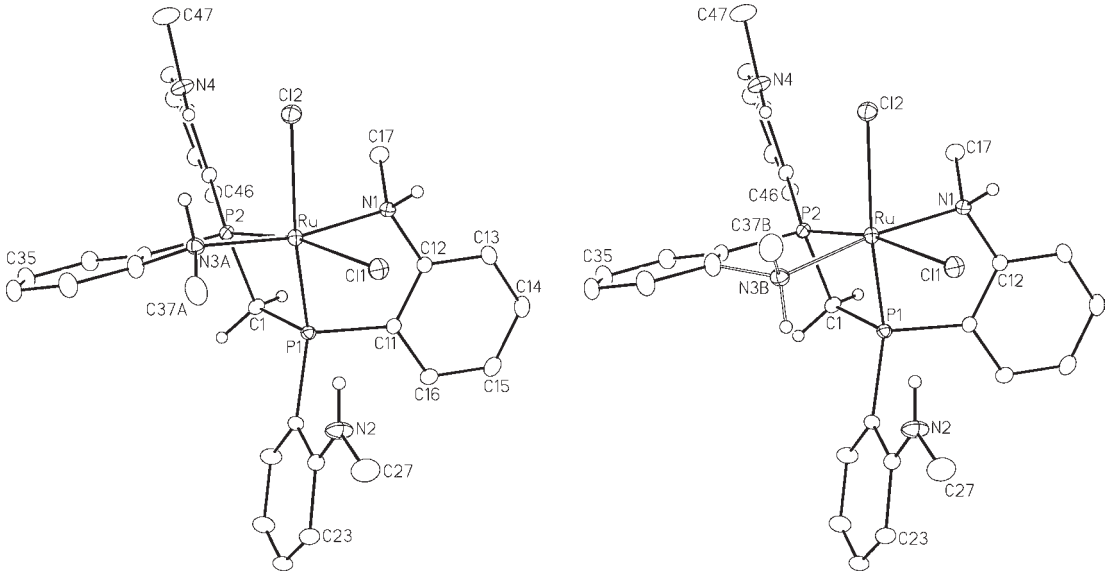

Figure 5. ORTEP diagrams of (left) the P_R,P'_R,N_R,N'_R and (right) P_R,P'_R,N_S,N'_R configurations of $[RuCl_2(P,P',N,N'\text{-mapm})]$ (**5**). Thermal ellipsoids as in Figure 1.

Scheme 5. Products of the Reaction between mapm and $[Ru(CO)_4(\eta^2\text{-}C_2H_4)]$ in Ambient Light

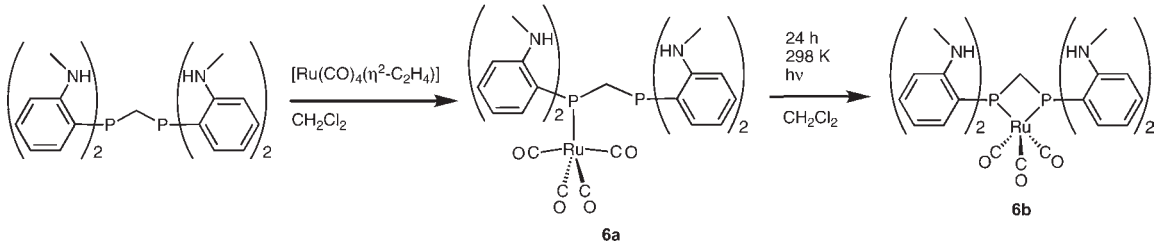

group (N(3A) and C(37A), Figure 5) implying co-crystallization of multiple stereoisomers (vide supra). The chelating geometry of the tetradentate, *P*,*P*′,*N*,*N*′-ligand at ruthenium is, to the best of our knowledge, unique. The strain of the four-membered chelate ring is made evident by compression of the P(1)−C(1)−P(2) angle from the ideal 109.5° to 91.09(9)° as well as compression of the P(1)−Ru−P(2) angle from the ideal 90° to 72.83(2)°. Within the five-membered *P*,*N*-chelate rings the angles are much less distorted with angles at Ru, P, N, and C close to the idealized values. All of the amine hydrogens come into reasonably close contacts (between 2.31 and 2.47 Å) with the two chloro ligands, which are less than the sum of the van der Waals radii[36] (3.05 Å) and suggest weakly attractive interactions.

The reaction of mapm with $[Ru(CO)_4(\eta^2\text{-}C_2H_4)]$ in dichloromethane solution initially produces $[Ru(CO)_4(P\text{-mapm})]$ (**6a**) which, at ambient temperature, over a 24 h period with exposure to ambient light, is completely converted to the thermodynamic product, $[Ru(CO)_3(P,P'\text{-mapm})]$ (**6b**, Scheme 5) by photolytic decarbonylation. The $^{31}P\{^1H\}$ NMR spectrum of the reaction mixture after a few hours of exposure to ambient light shows two doublets at δ_P 15.1 and −66.0 (d, $^2J_{PP}$ = 115 Hz) for the coordinated and pendent phosphines of **6a**, respectively, while the signal for **6b** shows up as a singlet at δ_P −41.3. The ^{31}P signal for the pendent end of the diphosphine of **6a** has an expectedly similar chemical shift to that of the free mapm ligand which appears at δ_P −60.9.[22] ^1H NMR analysis of **6a** shows two broad quartets at δ_H 4.65 and 4.19 corresponding to two chemically distinct pairs of amine hydrogens and were identified (by GCOSY analysis) as having vicinal relationships to the *N*-methyl protons which resonate at δ_H 2.74 and 2.54, respectively. The chemical shifts of the amine protons, which are close to that of the free ligand (δ_H = 4.62)[22] are consistent with pendent amine groups. The fact that only two methyl resonances are observed in the ^1H NMR spectrum of **6a** eliminates the possibility that the kinetic product is $[Ru(CO)_3(P,N\text{-mapm})]$, which would be expected to show four distinct *N*-methyl environments. The monodentate coordination mode of **6a** is analogous to that reported by Kiel and Takats for $[Ru(CO)_4(P\text{-dppm})]$ (dppm = $Ph_2PCH_2PPh_2$), which was found to undergo photodissociation, resulting in release of carbon monoxide and generating $[Ru(CO)_3(P,P'\text{-dppm})]$.[47] The methylene proton signal of **6a**, at δ_H 3.53, appears as a doublet of doublets because of coupling with two chemically inequivalent phosphorus nuclei. Although the $^{31}P\{^1H\}$ NMR spectrum of **6b** at ambient temperature appears as a singlet (vide supra), cooling to −80 °C results in splitting of this singlet resonance into two broad signals at −42.0 and −46.5, showing that the exchange of axial and equatorial phosphorus nuclei by a Berry-pseudorotation can be slowed to render them distinguishable at this temperature. ^1H NMR analysis of **6b** shows a broad quartet at δ_H

(47) Kiel, G.-Y.; Takats, J. *Organometallics* **1989**, *8*, 839–840.

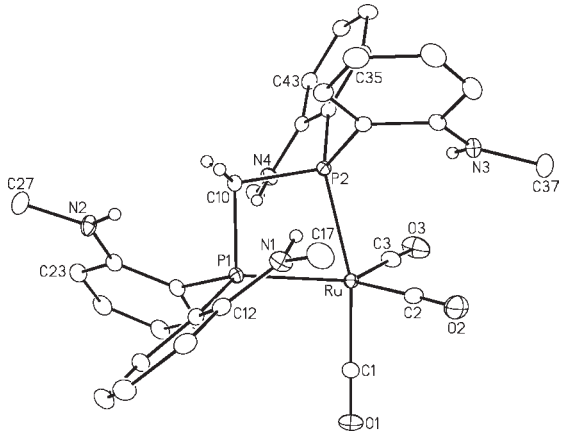

Figure 6. ORTEP diagram of $[Ru(CO)_3(P,P'\text{-mapm})]$ (**6b**). Thermal ellipsoids as in Figure 1.

4.95 ($^3J_{HH}$ = 5.2 Hz) representing the amine hydrogens, a triplet at 4.89 ($^2J_{PH}$ = 10.0 Hz) representing the methylene protons and a doublet at 2.59 ($^3J_{HH}$ = 5.2 Hz) representing the *N*-methyl protons. The chemical equivalence of these groups of protons at ambient temperature is consistent with a fluxional process.

X-ray crystallographic analysis of **6b** illustrates the pseudotrigonal bipyramidal geometry at ruthenium with clearly distinguishable axial and equatorial phosphine donors (Figure 6). The strain of the four-membered chelate ring is made evident by the P(1)−C(10)−P(2) and P(1)−Ru−P(2) angles of 97.32(10)° and 71.41(2)°, respectively, which are compressed from the idealized values of 109.5° and 90°, respectively. The chelate ring is exceptionally planar as is shown by the P(1)−Ru−P(2)−C(10) torsional angle of only 0.18(7)°, while the analogous torsional angles for the four-membered chelate rings of **4** and **5** are 16.9° and 7.23(7)°, respectively. Within the trigonal equatorial plane the angles (113.8(1)° to 129.55(9)°) deviate slightly from the idealized 120°, with the largest angle (P(1)−Ru−C(3)) appearing to have opened up to accommodate the pendent N(4) amine group which projects into this plane from above in Figure 6. As is typical for trigonal bipyramidal structures containing a chelate, the Ru−P(2) vector is tilted from the idealized axial orientation, owing to chelate ring strain, such that the P(2)−Ru−C(1) angle (166.34(7)°) deviates from the idealized 180°.

We attempted to exploit the pendent phosphine of **6a** to prepare a dinuclear ruthenium complex of the formulation $[Ru_2(CO)_x(\mu\text{-}P,P'\text{-mapm})]$ by reacting mapm with 2 equiv of $[Ru(CO)_4(\eta^2\text{-}C_2H_4)]$ in complete darkness (to prevent conversion of **6a** to **6b**). However, rather than producing the expected binuclear complex, this reaction generated a mixture, containing approximately equal concentrations of $[Ru_3(CO)_{10}(\mu\text{-}P,P'\text{-mapm})]$ (**7**) and **6a**, the latter of which was gradually converted to **6b** upon exposure to ambient light (Scheme 6) as determined by $^{31}P\{^1H\}$ and ^1H NMR spectroscopy. Washing with *n*-pentane easily removed **6b**, allowing **7** to be purified and crystallized for X-ray structural analysis. Complex **7** can also be prepared more directly by reacting mapm with 1 equiv of $[Ru_3(CO)_{12}]$ in tetrahydrofuran solution, and the mixture produced by this method is also spectroscopically devoid of **6b**. The $^{31}P\{^1H\}$ NMR spectrum of **7** shows only a singlet at δ_P 2.2, consistent with a symmetric bridging mode of the mapm ligand which serves to

Scheme 6

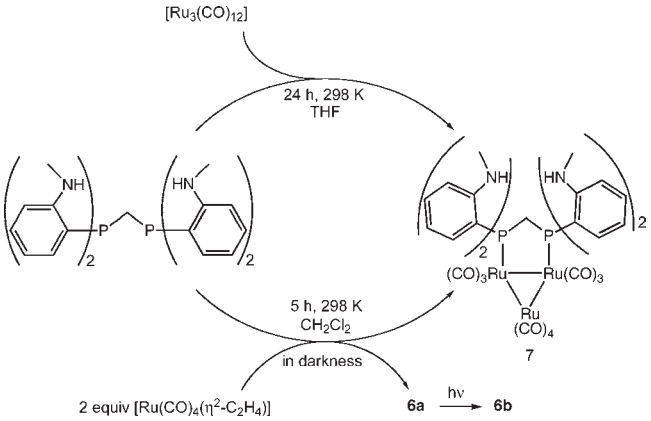

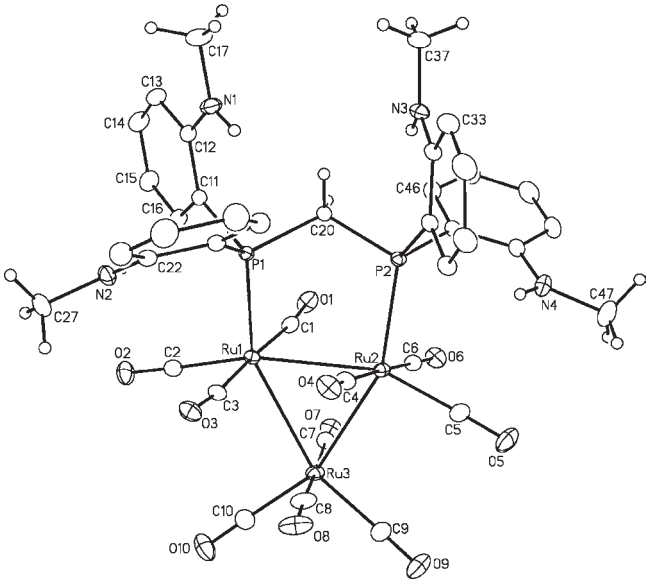

Figure 7. ORTEP diagram of $[Ru_3(CO)_{10}(\mu\text{-}P,P'\text{-mapm})]$ (**7**). Thermal ellipsoids as in Figure 1.

simplify the ^1H NMR spectrum, as does the fact that none of the amines participate in coordination. The methylene protons appear as a triplet at δ_H 4.76 while the amine hydrogen signal appears as a relatively upfield quartet at δ_H 3.94. Interestingly, the *N*-methyl proton signal appears as a slightly broadened doublet because of 2.5 Hz coupling with the amine hydrogen (a typical coupling constant in usually twice as large).[22] The slight broadening of this signal may be a consequence of the fluxionality of the carbonyl moieties on the trinuclear core which has been well documented within the analogous dppm-bridged system.[48] This fluxionality is made evident by the $^{13}C\{^1H\}$ spectrum, which shows only a single resonance at δ_C 210.9 representing all carbonyls. The infrared spectrum of **7** in CH_2Cl_2 is similar to that described for the dppm analogue[48] showing multiple carbonyl stretches between 2079 and 1955 cm^{-1}.

The solid state structure of compound **7** (Figure 7) clearly illustrates the *P*,*P*′-bridging mode of the mapm ligand across two ruthenium atoms, each of which possesses three terminally bound carbonyl ligands while

(48) Cotton, F. A.; Hanson, B. E. *Inorg. Chem.* **1977**, *16*, 3369–3371.

sharing a bridging $Ru(CO)_4$ unit. All Ru−Ru bond lengths are very similar (Ru(1)−Ru(2), 2.8464(3); Ru(2)−Ru(3), 2.8567(3); Ru(1)−Ru(3), 2.8504(3) Å) despite the presence of the bridging diphosphine across the Ru(1)−Ru(2) bond. As is typical in such clusters, pairs of carbonyls that are almost eclipsed when viewed along the metal−metal bonds are actually staggered slightly to avoid unfavorable contacts. As a result, the torsion angles of these carbonyls about Ru−Ru bonds vary between 15.7(1)° and 20.5(1)°.

The preparation of **7**, in which all amine groups were pendent, led us to ponder whether amine coordination could be induced. Decarbonylation of **7** was attempted by various methods including UV photolysis and carbonyl oxidation with one or more equivalents of trimethylamine-*N*-oxide. However, each of these attempts produced complex mixtures of unidentified products as was observed spectroscopically.

The previously reported dmapm analogue, $[Ru(CO)_3(P,P'\text{-dmapm})]$,[45] had previously been shown to act as a useful precursor for the synthesis of the heterobimetallic complex, $[RhRuCl(CO)_3(\mu\text{-}CO)(\mu\text{-}P,N,P',N'\text{-dmapm})]$; however, instability of the complex was believed to result from the substantial lability of the *N*,*N*-dimethylamino donors of the dmapm ligand. We thought that substituting dmapm by mapm within such a bimetallic complex might better stabilize the soft metal combination by providing less labile *N*-methylamino donors. However, an attempt to synthesize the heterobinuclear complex, $[RhRuCl(CO)_3(\mu\text{-}CO)(\mu\text{-}P,N,P',N'\text{-mapm})]$, from **6b** and 0.5 equiv of $[RhCl(\mu\text{-}Cl)(CO)_2]_2$ reveals a number of products by $^{31}P\{^1H\}$ NMR, which curiously includes the previously reported dirhodium species, $[Rh_2Cl_2(CO)_2(\mu\text{-}P,N,P',N'\text{-mapm})]$.[22]

Conclusions

A number of coordination modes for *ortho*-phosphinoaniline ligands at ruthenium have been reported herein and, as was previously described in related Rh chemistry,[22] the *N*-methyl and *N*,*N*-dimethyl analogues can give rise to rather different chemistries. For example, a comparison of the reactivities of the monophosphinoaniline ligands, Ph_2PAr and Ph_2PAr' (Ar = *o*-C_6H_4NHMe; Ar′ = *o*-$C_6H_4NMe_2$) with $[RuCl(\mu\text{-}Cl)(\eta^6\text{-}p\text{-cymene})]_2$ (**1**), illustrates that the degree of *N*-methyl substitution on the ligand influences the barrier to amine coordination. While the *N*,*N*-dimethyl complex, $[RuCl_2(\eta^6\text{-}p\text{-cymene})(P\text{-}Ph_2PAr')]$ (**3a**), rapidly undergoes amine coordination under mild conditions to afford the *P*,*N*-chelated $[RuCl(\eta^6\text{-}p\text{-cymene})(P,N\text{-}Ph_2PAr')]Cl$ (**3b**), the *N*-methyl analogue, $[RuCl_2(\eta^6\text{-}p\text{-cymene})(P\text{-}Ph_2PAr)]$ (**2a**), is stabilized by intramolecular hydrogen bonding in the monodentate *P*-coordinated isomer and requires kinetic assistance from a protic solvent to promote formation of the *P*,*N*-chelate, $[RuCl(\eta^6\text{-}p\text{-cymene})(P,N\text{-}Ph_2PAr)]Cl$ (**2b**). Compound **2b** can be deprotonated to yield the amido complex, $[RuCl(\eta^6\text{-}p\text{-cymene})(P,N\text{-}Ph_2PAr^-)]$ (**2c**), which appears to undergo enantiomerization in solution, presumably through the coordinatively unsaturated species, $[Ru(\eta^6\text{-}p\text{-cymene})(P,N\text{-}Ph_2PAr^-)]Cl$ (**2d**). Although **2c** has been shown to act as a ketone transfer hydrogenation catalyst, the mechanism remains unclear. We are currently attempting to isolate the amine-hydride complex, $[RuH(\eta^6\text{-}p\text{-cymene})(P,N\text{-}Ph_2PAr)]^+$, as well as the amido-hydrido complex $[RuH(\eta^6\text{-}p\text{-cymene})(P,N\text{-}Ph_2PAr^-)]$, to test their activities in ketone transfer hydrogenation catalysis.

Highly diverse coordination chemistry was observed using the related diphosphine ligands $Ar'_2PCH_2PAr'_2$ (dmapm) and $Ar_2PCH_2PAr_2$ (mapm). Whereas the dmapm ligand reacted with **1** to give the *P*,*P*′-chelate, $[RuCl(\eta^6\text{-}p\text{-cymene})(P,P'\text{-dmapm})]Cl$ (**4**), in which all dimethylanilinyl groups remained pendent, mapm reacted by displacement of the *p*-cymene group to give $[RuCl_2(P,P',N,N'\text{-mapm})]$ (**5**) in which both phosphorus and two of the *N*-methylanilinyl groups are bonded to Ru, giving an unprecedented coordination mode for the ligand. Complex **4** is believed to undergo an isomerization between a C_s-symmetric *P*,*P*′-chelate and a yet unidentified species in solution while complex **5**, which exhibits a *P*,*P*′,*N*,*N*′-chelation mode, is prepared as a mixture of stereoisomers. Starting from the Ru(0) precursor, $[Ru(CO)_4(\eta^2\text{-}C_2H_4)]$, the pendent chelate complex $[Ru(CO)_4(P\text{-mapm})]$ (**6a**) results from displacement of ethylene by mapm which, upon exposure to ambient light for an extended period, is eventually converted to **6b** via photodissociation of CO. Our attempts to prepare binuclear complexes of ruthenium bridged by the diphosphinoanilines, although unsuccessful, have resulted in the generation of the trinuclear compound $[Ru_3(CO)_{10}(\mu\text{-}P,P'\text{-mapm})]$ (**7**). None of the complexes **6a**, **6b**, nor **7** are found to possess coordinated aniline donors, and our attempts to displace carbonyl functionalities from compound **7**, to cleanly generate complexes stabilized by coordinated amines, were unsuccessful, presumably reflecting the lack of affinity of the soft Ru(0) center for the hard amine groups. Nevertheless, the pendent amines of complexes **6b** and **7** serve as potential stabilizing functionalities in the event of coordinative unsaturation at the metal centers.

Although the trinuclear dmapm complex, $[Ru_3(CO)_{10}(\mu\text{-}P,P'\text{-dmapm})]$, analogous to **7**, has not yet been synthesized, it can presumably be prepared in an analogous manner since amine coordination does not seem to have an influence on diphosphinoaniline reactivity with ruthenium carbonyl complexes. However, reactions of the monophosphinoanilines, Ph_2PAr and Ph_2PAr', with $[Ru(CO)_4(\eta^2\text{-}C_2H_4)]$ are expected to result in *P*,*N*-chelates, and synthetic investigations are currently underway to confirm this proposal.

Acknowledgment. We thank the Natural Sciences and Engineering Research Council of Canada (NSERC) and the University of Alberta for financial support for this research and NSERC for funding the Bruker PLATFORM/SMART 1000 CCD diffractometer, the Bruker D8/APEX II CCD diffractometer, and the Nicolet Avatar IR spectrometer. We thank the Department's Analytical and Instrumentation Laboratory, NMR Spectroscopy Laboratory, and Mass Spectrometry Facility for exceptional assistance, as well as Dr. Owen C. Lightbody and Dr. Jason Cooke for helpful discussions.

Supporting Information Available: Tables of crystallographic experimental details and selected bond lengths and angles for compounds **2a**, **2b**·C_4H_8O, **2c**, **3b**·$2CH_2Cl_2$,H_2O, **4**, **5**·$0.5CH_2Cl_2$, **6b**, and **7**·$0.5C_5H_{12}$,$0.5CH_2Cl_2$. Atomic coordinates, interatomic distances and angles, anisotropic thermal parameters, and hydrogen parameters for these compounds in a CIF file. This material is available free of charge via the Internet at http://pubs.acs.org.